Cell Motility and the Cytoskeleton 64:199–216 (2007)

Changes in Cholesterol Levels in the Plasma Membrane Modulate Cell Signaling and Regulate Cell Adhesion and Migration on Fibronectin

O. G. Ramprasad,[1] G. Srinivas,[1] K. Sridhar Rao,[1] Powrnima Joshi,[2] Jean Paul Thiery,[2] Sylvie Dufour,[2]* and Gopal Pande[1]*

[1]*Center for Cellular and Molecular Biology, Hyderabad, India*
[2]*UMR 144 CNRS, Institut Curie, Paris, France*

The number and distribution of lipid molecules, including cholesterol in particular, in the plasma membrane, may play a key role in regulating several physiological processes in cells. We investigated the role of membrane cholesterol in regulating cell shape, adhesion and motility. The acute depletion of cholesterol from the plasma membrane of cells that were well spread and motile on fibronectin caused the rounding of these cells and decreased their adhesion to and motility on fibronectin. These modifications were less pronounced in cells plated on laminin, vitronectin or plastic, indicating that cholesterol-mediated changes in adhesion and motility are more specific for adhesion mediated by fibronectin-specific integrins, such as $\alpha5\beta1$. These changes were accompanied by remodeling of the actin cytoskeleton, the spatial reorganization of paxillin in the membrane, and changes to the dynamics of $\alpha5$ integrin and paxillin-rich focal adhesions. Levels of tyrosine phosphorylation at position 576/577 of FAK and Erk1/Erk2 MAP-kinase activity levels were both lower in cholesterol-depleted than in control cells. These levels normalized only on fibronectin when cholesterol was reincorporated into the cell membrane. Thus, membrane cholesterol content has a specific effect on certain signaling pathways specifically involved in regulating cell motility on fibronectin and organization of the actin cytoskeleton. Cell Motil. Cytoskeleton 64:199–216, 2007.

Key words: integrin; lipids; migration; adhesion; actin; extracellular matrix; FAK; Erk1/Erk2 MAP-kinase

INTRODUCTION

The relationship between cell adhesion, cell shape and cell locomotion is of considerable interest in cell biology. These three processes are initiated by independent stimuli, and regulated by different mechanisms. They are, however, intricately interlinked, because their regulation involves many common signaling pathways and molecular assemblies with structural and functional similarities. Integrins are among the most important molecules influencing all the three processes. These proteins that bind to and get activated by the extracellular matrix (ECM) lead to the assembly of a large number of cyto-

This article contains supplementary material available via the Internet at http://www.interscience.wiley.com/jpages/0886-1544/suppmat.

Powrnima Joshi's present address is Department of Neurology, Yale University School of Medicine, New Haven, CT 06520-8018, USA.

Jean Paul Thiery's present address is IMCB PROTEOS 6-03, 61 Biopolis Drive, 138673, Singapore.

Contract grant sponsor: CNRS; Contract grant sponsor: Indo-French Center for the Promotion of Advanced Research (IFCPAR); Contract grant number: 2303-4.

*Correspondence to: Gopal Pande, Center for Cellular and Molecular Biology, Uppal Road, Hyderabad 500 007, India. E-mail: gpande@ccmb.res.in or Dr. Sylvie Dufour, UMR 144 CNRS, Institut Curie, 75248 Paris Cedex 05, France. E-mail: Sylvie.Dufour@curie.fr

Received 26 May 2006; Accepted 2 November 2006

Published online 19 January 2007 in Wiley InterScience (www.interscience.wiley.com).
DOI: 10.1002/cm.20176

plasmic signaling molecules [Giancotti and Ruoslahti, 1999; Zamir and Geiger, 2001; Hynes, 2002]. The integrin-mediated organization of the actin-based cytoskeleton in cells is a highly efficient process [Blystone, 2004]. The formation of this cytoskeleton is also controlled by small GTPases in the cytoplasm, such as rho, rac and cdc42, which organize actin into stress fibers, lamellipodial and filopodial structures, respectively [Manneville and Hall, 2002]. Reorganizations of the structure and distribution of actin play a key role in regulating the shape, adhesion and motility of cells [Ingber, 2003a]. Thus, factors affecting the actin-based cytoskeleton are also potential regulators of cell shape, adhesion and motility.

Actin cytoskeleton formation is a dynamic process, because actin polymerizes and depolymerizes according to cell activation state [Ridley et al., 2003; Giannone et al., 2004]. Thus, flattened cells (and fibroblasts in particular) have robust actin stress fibers crisscrossing the length and breadth of the cell. Motile cells form large numbers of lamellipodia, which are free of stress fibers and have a submembranous mesh-like organization of F-actin [Small et al., 2002]. Less flattened and rounded cells display no stress fiber formation and have more cortically organized F-actin. These cells have no lamellipodial or filopodial extensions and are less motile [Rafelski and Theriot, 2004]. The role of focal adhesion kinase (FAK) in actin cytoskeleton formation and cell motility is well documented. FAK affects motility by regulating the activity of Rho family GTPases, GTPase-activating proteins, guanine nucleotide exchange factors and Erk1/2 MAP kinases [Schlaepfer and Mitra, 2004; Mitra et al., 2005]. FAK also regulates the formation of filopodia and lamellipodia by means of differential binding to paxillin (Pax) [Schaller, 2004]. Pax can regulate cell motility independently, based on its precise location with respect to the center and periphery of cells [Zamir et al., 2000], differential phosphorylation at tyrosine and serine/threonine residues [Brown and Turner, 2004] and association with other kinases [Bokoch, 2003]. Thus, FAK and/or Pax may play a significant role in regulating cell shape and motility.

It has been suggested that membrane lipids influence or are influenced by FAK and Pax activities. Phosphoinositides in the cytoplasm and submembranous zones, the levels of which are regulated by phosphoinositol-di-phosphate kinases (PIP_2-K), may play a key role in this process [Ling et al., 2002]. The direct association of soluble and membrane-bound lipid molecules, such as palmitic acid, with integrins and/or integrin-associated proteins (IAPs), such as tetraspanins, has been demonstrated [Claas et al., 2001; Yang et al., 2004]. Cholesterol (chol), a lipid present in the cell membrane, has been shown to affect integrin functions, such as cell adhesion and the growth of transformed and normal cells, although the mechanisms involved remain unclear [Gopalakrishna et al., 2000, 2004; Pande, 2000; Kaur et al., 2004]. Chol has also been reported to regulate the actin cytoskeleton via PIP_2-K and Wiskott-Aldrich Syndrome Protein [Manes and Martinez, 2004], and to regulate endothelial cell motility and membrane microviscosity [Ghosh et al., 2002] but, again, the underlying molecular mechanisms remain unclear. The shape and curvature of membranes, which depends on the presence of chol in the membrane [Chen and Rand, 1997; Rukmini et al., 2001], may regulate gene expression profiles and the activities of intracellular signaling molecules [Ingber, 2003b]. It is therefore important to determine the effects of membrane chol levels on specific signaling molecules involved in regulating cell shape and motility.

We studied the shape, adhesion and motility of L27 cells. These cells are derived from the highly deformable and motile mouse sarcoma S180 cell line, which expresses several integrins and adheres to various ECM components, but spreads and migrates preferentially on fibronectin (FN)-coated surfaces [Beauvais et al., 1995]. The elimination of chol from the plasma membrane caused L27 cells to become more rounded and decreased their adhesion to the substratum. In some cases, cell motility was also reduced. These changes in the morphology, adhesion and motility of cells were partially or almost fully reversible, depending on the nature of the substratum, indicating that the changes resulting from chol depletion preferentially affected FN-dependent adhesion. The modification of membrane chol content also affected the actin-cytoskeleton network, and altered the dynamics of α5 integrin and Pax-rich focal adhesions and the tyrosine phosphorylation of FAK and p44/42 MAP kinase.

MATERIALS AND METHODS

Reagents, cDNA and Antibodies

Methyl-β-cyclodextrin (MBCD) and chol-loaded MBCD (CHO-MBCD) complex were obtained from Cyclodextrin Technologies Development Inc., USA. Cholesterol oxidase was purchased from Sigma. Horseradish peroxidase (HRP) was obtained from Bangalore Genei India Ltd. Protein-A-Sepharose beads and Lipofectamine Plus™ reagents were obtained from Amersham Biosciences and Invitrogen, respectively. The α5-GFP integrin expression plasmid was generously provided by Alan F. Horwitz (University of Virginia at Charlottesville, USA). The mammalian expression plasmid for GFP-Pax was kindly donated by K.M. Yamada. Rhodamine-phalloidin was purchased from Molecular Probes. The p44/42 MAP kinase activity assay kit was obtained from Cell Signaling Technology. The BM Chemiluminescence Western Blotting kit was purchased from Roche. The primary antibodies used are listed in supplementary Table I.

Cell Lines

All experiments were carried out with L27 cells. These cells are derived from the mouse S180 sarcoma cell line and stably express human α5 integrin. Another cell line, D711, also derived from S180 but expressing high levels of human α4 integrin, was used as the control cell line. The creation and properties of these cell lines have been discussed elsewhere [Beauvais et al., 1995].

Cell Cultures and Membrane Chol Depletion and Restoration

The cells were cultured in DMEM (Sigma) supplemented with 10% FCS (Sigma and Invitrogen), streptomycin (50 μg/ml) and penicillin (60 μg/ml). The cells were grown in a chamber containing 5% CO_2/95% air, maintained at 37°C. Chol was depleted from the plasma membrane by starving the cells of serum for two hours in DMEM and treating them with 10 mM MBCD in serum-free DMEM for 1 h. Membrane chol levels were restored by eliminating MBCD from the medium by washing the cells with serum-free DMEM and then treating the cells with CHO-MBCD in serum-free DMEM (100 μM Chol component) for 2–4 h.

Biochemical Estimation of Membrane Chol

Membrane chol levels were determined with a modified version of a previously described microenzymatic fluorescence assay [Gopalakrishna et al., 2000]. This method included treatment with cholesterol oxidase, to ensure the exclusive determination of free chol present in the plasma membrane, and not of chol esters present in the cytoplasm. Briefly, $2 \times 10^6 - 3 \times 10^6$ untreated, MBCD-treated or CHO-MBCD-treated cells were washed at several time points with cold 0.1 M potassium phosphate buffer and scraped off the substratum with a rubber policeman, on ice. The cells were then sonicated in a Branson sonicator and centrifuged. An aliquot of the supernatant equivalent to 1×10^5 cells was assayed. The assay mixture consisted of 1 U/ml cholesterol oxidase, 10 U/ml horse-radish peroxidase (HRP), 0.5% Triton-X 100, 20 mM sodium cholate, 4 mg/ml para-hydroxy-phenyl acetic acid in 0.1 M potassium phosphate buffer. The supernatant sample was incubated with the assay mixture at 37°C for 1 h, and fluorescence was quantified in a Hitachi-F-4010 spectrofluorimeter (excitation 325 nm and emission 415 nm). The chol content of cells was determined from a standard curve.

Coating of the Substratum and Cell Adhesion Assay

Tissue culture dishes, bacteriological Petri dishes or coverslips were coated with various concentrations of FN, laminin I (LN) or vitronectin (VN), either at 37°C for 2 h, or at 4°C overnight, as previously described [Dufour et al., 1999]. For adhesion assays, chol was depleted and restored as described above. The cells were plated on the coated substrata in serum-free DMEM. However, for uncoated plastic, we used DMEM supplemented with 10% FCS and, after the cells had spread, the medium was replaced with serum-free DMEM for further treatments. We estimated the percentage of adherent cells as previously described [Beauvais et al., 1995]. Negative control values were obtained with cells plated on BSA and the reference point (100%) for cell adhesion was calculated from cells plated on polylysine. At least three independent experiments were carried out for each substratum concentration and for each cell type.

Time-Lapse Video Microscopy

Cells in serum-free DMEM were plated on FN- or LN- or VN-coated dishes or on tissue culture dishes and incubated for 2 h. The dishes were placed on the motorized stage of a computer-controlled epifluorescence microscope (Leica DMRBE) equipped with an enclosed warming incubator, a cooled CCD camera (Princeton RTE/CCD) and a PC workstation. The enclosed incubator made it possible to maintain the sample at 37°C in a humidified atmosphere containing 6% CO_2/94% air. Metamorph software (Universal Imaging) was used to control image acquisition with a 20× phase objective. Images were recorded at the rate of one per minute. Images were acquired simultaneously from several fields and through the sequential treatment of cells with control medium (serum-free DMEM) for 1 h and 10 mM MBCD for 1 h. MBCD was then replaced by CHO-MBCD and image acquisition continued for 3–4 h. Cell movements were tracked and analyzed with Metamorph software. At least 20 cells were analyzed in each field and three independent experiments were carried out. Adobe Premiere (Version 6.0) software was used to reconstruct movies of cell motility, by assembling the images in order.

Fluorescently tagged proteins in living cells were visualized as follows: 1.5×10^5 cells in 35 mm culture dishes were transiently transfected with 10 μg Lipofectamine Plus and 2 μg of DNA (expression plasmids for α5 integrin-GFP or GFP-Pax), according to the manufacturer's instructions. After two days, the cells were dissociated and plated on 5 μg/ml FN-coated coverslips, 2 h before video microscopy. GFP-fluorescence images were acquired from untreated cells for 1 h (images recorded every 30 sec, using a 100× objective). Cells were then treated with 10 mM MBCD for 1 h, with images recorded every 30 sec during the treatment. Cells were then treated with CHO-MBCD and image acquisition was continued at 30-sec intervals for Pax-GFP and α5-GFP, over a period of 2 h.

Fluorescence Microscopy of Cells

Cells plated on uncoated or FN- or LN-coated coverslips were fixed with formaldehyde and immunostained as previously described [Dufour et al., 1999; Chu et al., 2004]. Preparations were viewed by epifluorescence microscopy, using a 63× objective on a Leica DMRBE microscope equipped with a cooled CCD camera (Hamamatsu C5985). Images were acquired with IP-Lab software or by TCS4D confocal microscopy with a DM microscope interfaced with an argon/krypton laser.

F-actin was stained with rhodamine-phalloidin as previously described [Gopalakrishna et al., 2004], and images were visualized with a Zeiss Axioplan2 microscope fitted with a 100× objective and the Apotome® module, using Zeiss Axiovison software.

Cell Surface labeling, Immunoprecipitation and Western Blotting

Subconfluent cell monolayers were surface-labeled with ^{125}I (Amersham) and proteins were extracted as previously described [Rossino et al., 1990; Beauvais et al., 1995].

Proteins were extracted from cell monolayers ($6 \times 10^6 - 7 \times 10^6$ cells) on ice. Cells were lysed in 1 ml of ice-cold lysis buffer, containing 50 mM Tris-HCl (pH 7.4), 150 mM NaCl, 2 mM NaF, 1 mM EDTA, 1 mM EGTA, 1 mM $NaVO_3.H_2O$ supplemented with 20 μg/ml each of aprotinin and leupeptin, 1 mM PMSF and 1% Triton-X 100. The lysates were kept on ice for 30 min, sonicated with a Branson sonicator, passed through 28G needles 5 times, and centrifuged. The protein content of the supernatant was determined by BioRad protein assay. For western blotting, the lysate (equivalent of 25 μg total protein) was boiled in SDS sample buffer and analyzed by SDS-PAGE. The proteins were then transferred onto membranes by electroblotting. For immunoprecipitation, lysate (equivalent of 200 μg of total protein) was incubated with anti-Pax antibody and the immunoprecipitate was immunoblotted with a pan-phosphotyrosine antibody. Western blots were incubated with specific primary antibodies, washed and then incubated with the anti-mouse IgG-POD/anti-rabbit IgG-POD labeled secondary antibody. Bands were detected by incubation with the BM chemiluminescence substrate. Bands were analyzed by densitometry with the Syngene gel documentation system. Western blots and immunoprecipitations were carried out in triplicate to ensure reproducibility.

Sucrose Density Gradients

L27 cells ($5 \times 10^6 - 6 \times 10^6$) plated on FN for 2 hrs or MBCD-treated cells or CHO-MBCD treated cells were lysed on ice using lysis buffer containing 1% Triton-X 100 (lysis buffer composition and lysate preparation are described in the previous paragraph). We mixed 0.9 ml of cell lysate with 0.9 ml of 90% sucrose to generate a 1.8 ml solution containing 45% sucrose. This solution was dispensed into a 4.2 ml Beckman polyallomer centrifuge tube. It was overlaid with 1.2 ml of 35% sucrose in lysis buffer, which was itself overlaid with 1 ml of 5% sucrose in lysis buffer. The sucrose gradients were prepared at 4°C. They were then centrifuged at 45,000 rpm in a Beckman SW60Ti rotor for 21 h at 4°C. We then collected 10 fractions of 400 μl each, on ice.

We analyzed the distribution of α5 integrins in the gradient fractions, by diluting 50 μl of each gradient fraction in lysis buffer without detergent, clearing it with protein-A-Sepharose beads and then subjecting it to immunoprecipitation with anti-α5-integrin antibody. The beads were washed and boiled in 1× SDS non-reducing sample buffer without 2-mercaptoethanol. Equal volumes of each fraction were analyzed by SDS-PAGE in a 9% acrylamide gel, followed by western blotting with anti-α5-integrin antibody. The distribution of Pax in gradient fractions was investigated by boiling equal volumes of each fraction in 3× SDS-sample buffer with 2-mercaptoethanol and immunoblotting with the anti-Pax antibody.

MAP Kinase Assay

MAP kinase assays were carried out with a kit, according to the manufacturer's instructions. The MAP kinase activity of cells plated on FN and LN was quantified by selectively immunoprecipitating active MAP kinase from cell lysates, using a Mab directed against p44/42 MAP kinase. The resulting immunoprecipitate was then incubated with an Elk-1 fusion protein, making it possible for the immunoprecipitated active MAP kinase to phosphorylate Elk-1 at Ser383. Elk-1 phosphorylation was then assessed by western blotting, using an antibody directed against phospho-Elk-1 (Ser383). On VN, MAP kinase activity was assessed by determining the level of

Fig. 1. Plasma membrane cholesterol content of L27 cells and the adhesion of these cells to FN, LN or VN after MBCD and CHO-MBCD treatment. (**A**) Changes in membrane chol content (mean values from 4 experiments ± s.d.) of L27 cells at various time points after MBCD and CHO-MBCD treatment. After 60 min of MBCD treatment, chol levels had fallen to 23% those in the corresponding control. The restoration of chol levels (with CHO-MBCD treatment, using 100 μM chol) was seen after 2 h in L27 cells. FACS profile of α5 integrin (**B**) or activated β1 integrin expression (**C**) in untreated L27 cells (white peaks) or MBCD-treated L27 cells (black peaks) for 45 min. (**D–L**), L27 cell adhesion to FN (white bars), LN (black bars) and VN (gray bars) in control conditions (D, G, J), and after MBCD (E, H, K) and CHO-MBCD (F, I, L) treatment.

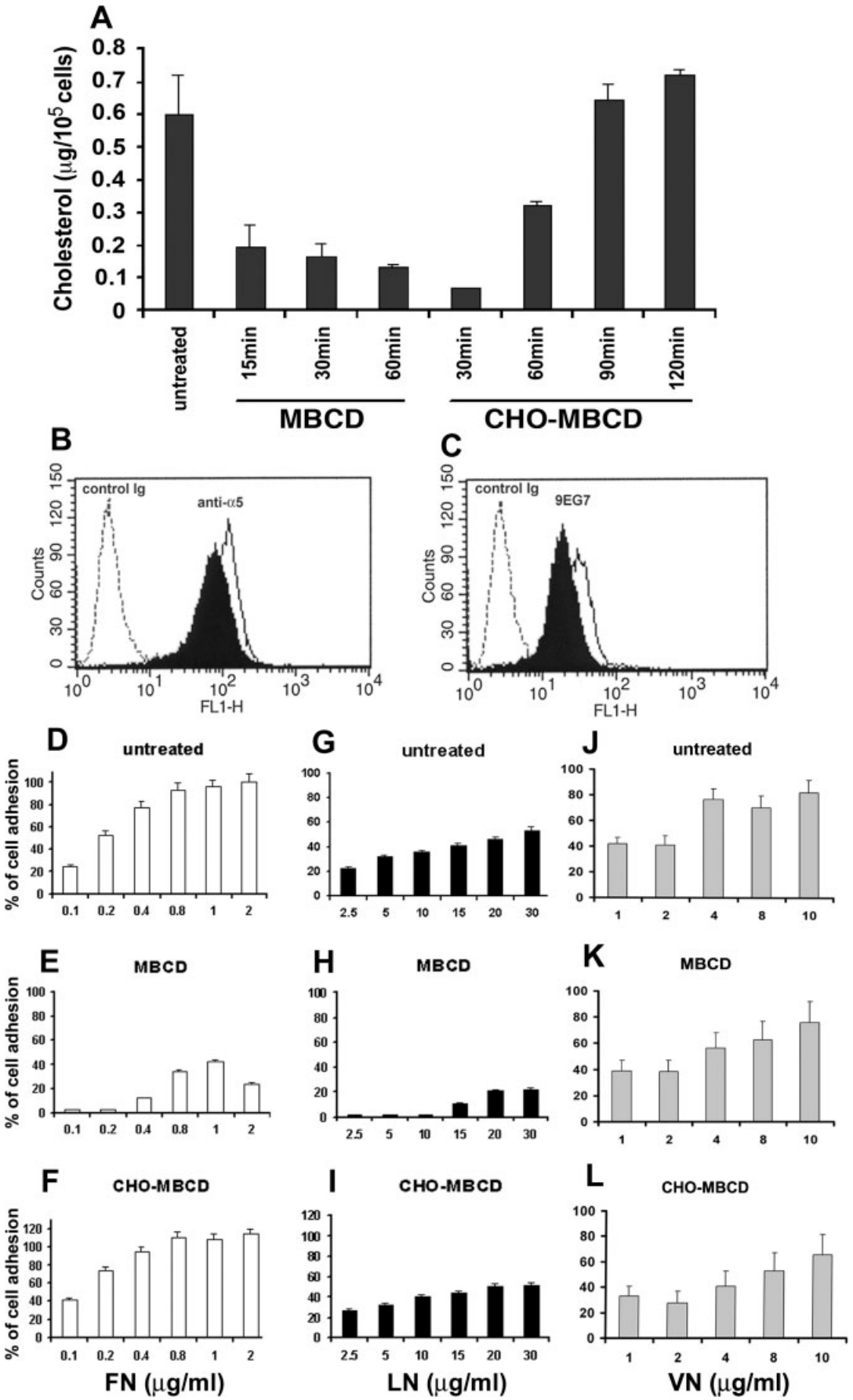
A
Cholesterol (μg/10^5 cells)
0.8
0.7
0.6
0.5
0.4
0.3
0.2
0.1
0
untreated
15min
30min
60min
30min
60min
90min
120min
MBCD
CHO-MBCD
B
control Ig
anti-α5
Counts
FL1-H
C
control Ig
9EG7
Counts
FL1-H
D
untreated
G
untreated
J
untreated
E
MBCD
H
MBCD
K
MBCD
F
CHO-MBCD
I
CHO-MBCD
L
CHO-MBCD
% of cell adhesion
FN (μg/ml)
LN (μg/ml)
VN (μg/ml)

Figure 1.

p44/p42 MAP kinase phosphorylation, by the direct western blotting of lysates with a monoclonal antibody against phospho-p44/42.

RESULTS

Integrin Expression in Cells

We chose to analyze L27 cells (a stably transfected clone derived from mouse sarcoma S180 cells) because these cells migrate well on FN-coated substrates. They also migrate in complex environments in vivo [Erickson et al., 1980], displaying migratory behavior similar to that observed for neural crest cells, an important embryonic cell population with strong migration potential. These cells therefore constitute a model system for cell motility. They produce endogenous α3, α5, α6, αV, β1 and β3 integrin subunits (supplementary data S2A), but do not express α1, α2 and α4 integrin subunits. They also express human α5 integrin, and have total α5 integrin levels five times higher than those in the parental S180 cells (supplementary data S2B). We have previously reported that α5β1 integrin expression in L27 cells increases the spreading and migration of these cells in vitro and in vivo. By contrast, the expression of another FN-specific integrin, α4β1 (the D711 clone), increases migration on FN-coated substrates in vitro, but has no effect on cell spreading [Beauvais et al., 1995].

Modulation of the Chol Content of the Membrane Affects Cell Adhesion

We used MBCD treatment to remove chol from the plasma membrane of cells. We then incubated cells with CHO-MBCD to restore chol levels in the membrane. Membrane chol levels decreased rapidly in L27 cells, following MBCD treatment (Fig. 1A), but were restored more slowly, eventually reaching levels similar to those in untreated cells. Similar results were obtained for D711 cells, except that the restoration was faster, with untreated levels reached within 60 minutes (supplementary data S3B).

We performed adhesion assays for cells with different levels of membrane cholesterol to see the adhesion and specific interaction of α5β1 or α4β1 expressing cells to different substrata. L27 cells adhered to FN-, LN- and VN-coated substrates in a dose-dependent manner. They adhered more efficiently to FN than to LN or VN; at the plateau, more than 95% cells adhered to FN (2 μg/ml) whereas only 50 % of L27 cells adhered to 30 μg/ml LN and 81% to 10 μg/ml VN (Figs. 1D, 1G and 1J). At low coating concentrations, levels of adhesion to FN, LN and VN were similar.

The elimination of chol from the cell membrane had a substrate-specific effect on adhesion (Figs. 1E, 1H and 1K). The level of adhesion of L27 cells to FN (2 μg/ml) was only one quarter that of untreated cells. The decrease in cell adhesion was smaller on LN (30 μg/ml; adhesion levels about half those before chol elimination) and no significant decrease in adhesion was observed on VN (10 μg/ml).

The restoration of membrane chol levels completely restored L27 cell adhesion on FN and LN after 2 h of CHO-MBCD treatment (Figs. 1F and 1I). Furthermore, L27 cells adhered more efficiently to FN after chol restoration than the untreated cells, at all the concentrations tested.

We assessed the effects of chol depletion on integrin expression and activation at the cell surface, using the relevant antibodies and flow cytometry. The levels of α5 (Fig. 1B) and activated β1 chain (Fig. 1C), α6 and αV (not shown) integrins were only slightly lower in MBCD-treated cells than in the control.

Thus, cell adhesion to FN is more strongly affected by the elimination and restoration of membrane chol than is cell adhesion to LN or VN. We then tried to identify the FN-specific integrins (α5β1 and α4β1 integrins) involved in the differential cell adhesion response to chol modulation. We compared the adhesion properties of L27 cells (which have high levels of α5β1 but no α4β1 integrin) with those of D711 cells (which have low levels of α5β1 and high levels of α4β1 integrin; supplementary data S3A). Chol depletion had no significant effect on D711 cell adhesion to FN (supplementary data S3C-E), in contrast to what was observed with L27 cells (Figs. 1D–1F). Thus, the modulation of chol levels preferentially affects α5β1-mediated cell adhesion to FN rather than adhesion through other integrins.

The Modulation of Membrane Chol Content Affects Cell Motility

Cell motility assays were performed on L27 cells plated on uncoated plastic (PL) or on PL coated with FN, LN or VN, and the velocity of cell movement under various membrane chol content conditions was calculated (Fig. 2A).

L27 cells were highly motile (80 μm/h; Fig. 2A, white bars) and well spread on FN (Fig. 2B, subpanel a). However, the elimination of chol from these cells slowed their movement (29 μm/h), and this slowing persisted even after 1 h of CHO-MBCD treatment, by which time chol levels in the membrane had already begun to recover (compare this time point in Fig. 1A). The treatment of L27 cells with MBCD resulted in rounding, but the cells spread more gradually during the restoration of chol levels in the membrane (Fig. 2B, subpanel b-d and Movie in supplementary data S4). Thus, changes in membrane chol levels induced changes in cell motility only after a lag period, during which time cell shape and

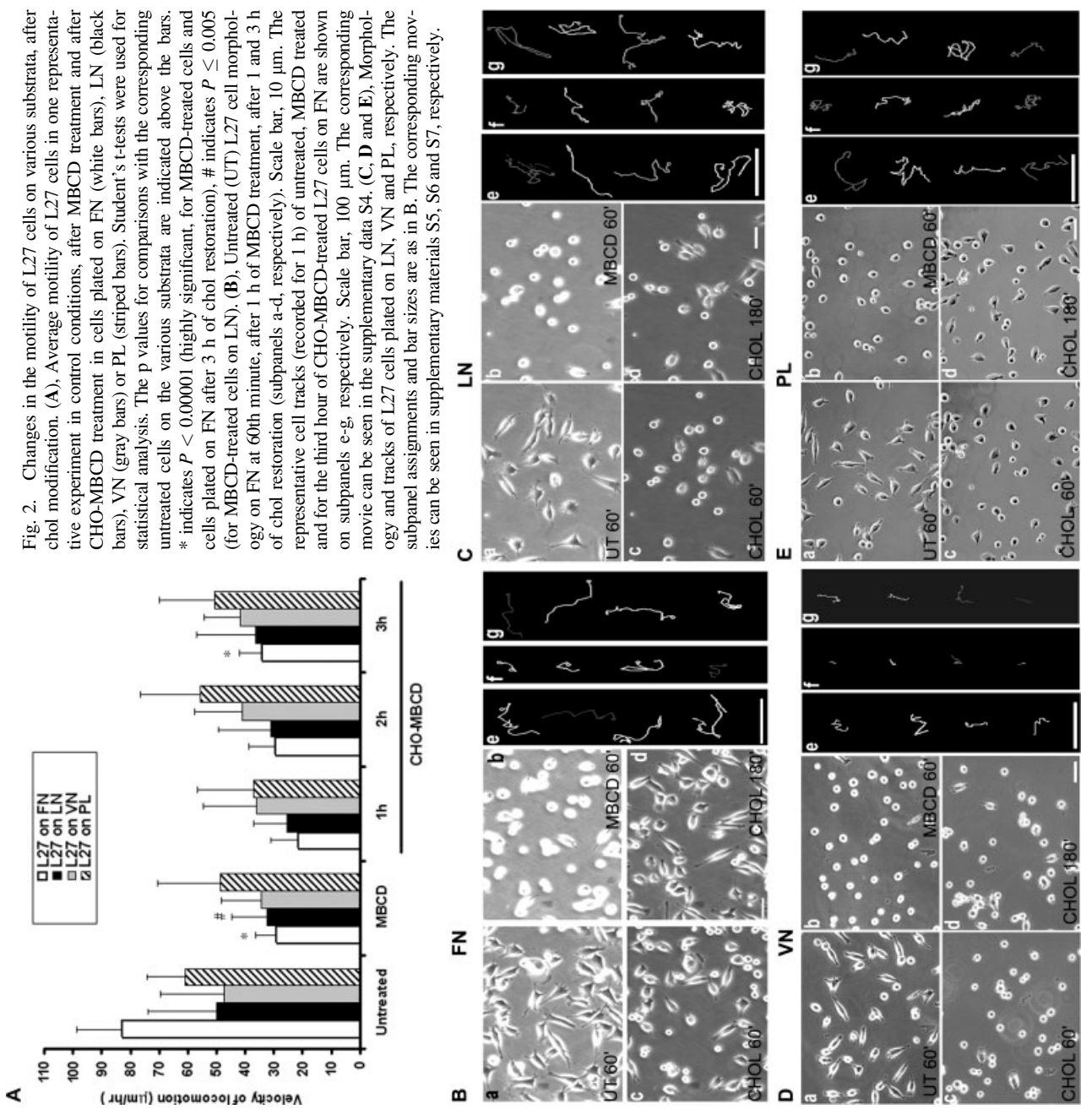

Fig. 2. Changes in the motility of L27 cells on various substrata, after chol modification. (**A**), Average motility of L27 cells in one representative experiment in control conditions, after MBCD treatment and after CHO-MBCD treatment in cells plated on FN (white bars), LN (black bars), VN (gray bars) or PL (striped bars). Student's t-tests were used for statistical analysis. The p values for comparisons with the corresponding untreated cells on the various substrata are indicated above the bars. * indicates $P < 0.00001$ (highly significant, for MBCD-treated cells and cells plated on FN after 3 h of chol restoration), # indicates $P \leq 0.005$ (for MBCD-treated cells on LN). (**B**), Untreated (UT) L27 cell morphology on FN at 60th minute, after 1 h of MBCD treatment, after 1 and 3 h of chol restoration (subpanels a-d, respectively). Scale bar, 10 μm. The representative cell tracks (recorded for 1 h) of untreated, MBCD treated and for the third hour of CHO-MBCD-treated L27 cells on FN are shown on subpanels e-g, respectively. Scale bar, 100 μm. The corresponding movie can be seen in the supplementary data S4. (**C**, **D** and **E**), Morphology and tracks of L27 cells plated on LN, VN and PL, respectively. The subpanel assignments and bar sizes are as in B. The corresponding movies can be seen in supplementary materials S5, S6 and S7, respectively.

motility signaling responses may have been activated. Furthermore, L27 cells recovered about 50% of their original speed after about 3 h of chol restoration, and were well spread on the substratum at this time point (Fig. 2B, subpanel d). Representative tracks of L27 cells followed for 1 h in control, MBCD and CHO-MBCD (during the 3rd hour of recovery) media, are shown in Fig. 2B, subpanels e–g. Chol-depleted L27 cells displayed a significant loss of cell motility on FN that was not restored to original levels following the restoration of membrane chol levels. By contrast, adhesion to FN and the original shape of the cells were restored.

The speed of movement of L27 cells plated on LN decreased by 36% ($P \leq 0.005$) after the removal of chol (Fig. 2A, black bars). A much larger and highly significant decrease (65%) was recorded for cells plated on FN. After 3 h of chol restoration, cell motility on LN had almost returned to the level for untreated cells. L27 cells plated on VN or on uncoated PL showed no significant change in the speed of cell locomotion after the removal or restoration of chol (Fig. 2A, gray and hatched bars, respectively). L27 cells plated on LN, VN and PL became more rounded after the removal of chol and only partially recovered their initial shape when membrane chol levels were restored (Figs. 2C–2E and movies in supplementary data S5, S6 and S7, respectively). Mean cell velocity was similar under the various treatments on VN or PL, but greater differences in cell velocity were observed on these surfaces than on FN (compare the standard deviation bar in Fig. 2A). Furthermore, MBCD treatment greatly decreased the total distance moved by the cells on VN (Fig. 2D, subpanel f), whereas the distance moved on LN and uncoated PL was similar to that on FN (Figs. 2B, 2C and 2E, subpanel f). Thus, the modulation of membrane chol levels specifically affects the direction of cell movement on VN-coated surfaces.

Thus, chol-dependent changes in L27 cell shape and motility were significant when these cells were plated on FN whereas changes were less marked, particularly for cell motility, on LN, VN and uncoated PL. By contrast, D711 cell motility was not significantly affected, on any substratum, by changes in chol levels in the cell membrane (supplementary data S8A).

Changes in Actin Cytoskeleton Organization

The observed changes in cell shape, substrate-specific spreading and the speed of cell locomotion are related to reorganization of the actin cytoskeleton. Untreated L27 cells on FN had large lamellipodia and a well organized robust network of actin filaments criss-crossing the cytoplasm (Fig. 3A). Cells plated on LN and VN had a less dense actin filament network than cells plated on FN (Figs. 3D and 3G). Cells put out larger numbers of filopodial projections on LN, whereas small lamellipodial extensions of the membrane were observed on VN. On PL, cells had thick stress fibers, correlated with their lower motility (Fig. 3J).

Following chol elimination from the membrane, the actin network became disorganized on FN, LN and VN, and even cortical actin was only weakly stained (Figs. 3B, 3E and 3H). On PL, the de-polymerization of actin after treatment was less extensive than that seen on FN and LN and some stress fibers were observed despite the rounding of the cell (Fig. 3K). The F-actin network reformed, and resembled that in untreated cells, when membrane chol levels were restored, on FN, LN, VN and PL (Figs. 3C, 3F, 3I and 3L).

Changes in the Phosphorylation of Pax and FAK and in MAP Kinase Activation in Chol-Deprived Cells

ECM proteins and intracellular signaling molecules are known to control actin cytoskeleton organization and thus to affect the motility of cells on different surfaces [Geiger et al., 2001]. The main molecules involved in signaling in this process are MAP kinase Erk1/2, Pax and FAK.

FAK levels were similar before and during chol elimination and after chol restoration in L27 cells, on all surfaces (Figs. 4A and 4B). MBCD decreased levels of P-Y925 and P-Y576/Y577 FAK in cells plated on FN (Figs. 4A, 4D and 4E, white bars). Pax phosphorylation on FN was not affected by MBCD treatment, but increased following chol restoration (Figs. 4A and 4G, white bars). The opposite pattern of phosphorylation was observed if these cells were plated on LN or VN: MBCD increased P-Y576/Y577 FAK levels (with the appearance of an extra band) in cells plated on LN, but not in those plated on VN, whereas Pax phosphorylation decreased in cells plated on LN (Figs. 4A, 4E and 4G respectively, black bars). After the restoration of chol levels, Y576/Y577 FAK phosphorylation returned to basal levels, but Pax phosphorylation remained low on LN.

Y397 FAK phosphorylation levels were similar in untreated and MBCD-treated cells on FN, but decreased

Fig. 3. Changes in the actin cytoskeleton of L27 cells on different substrata. Fluorescence images showing the F-actin filaments of L27 cells plated on FN (**A–C**), LN (**D–F**), VN (**G–I**) or PL (**J–L**) in control (A, D, G and J) conditions, after 1 h of MBCD treatment (B, E, H and K) and 2 h of CHO-MBCD treatment (C, F, I and L). The images were taken on a plane 0.35 μm above the base of each cell. Bar, 10 μm.

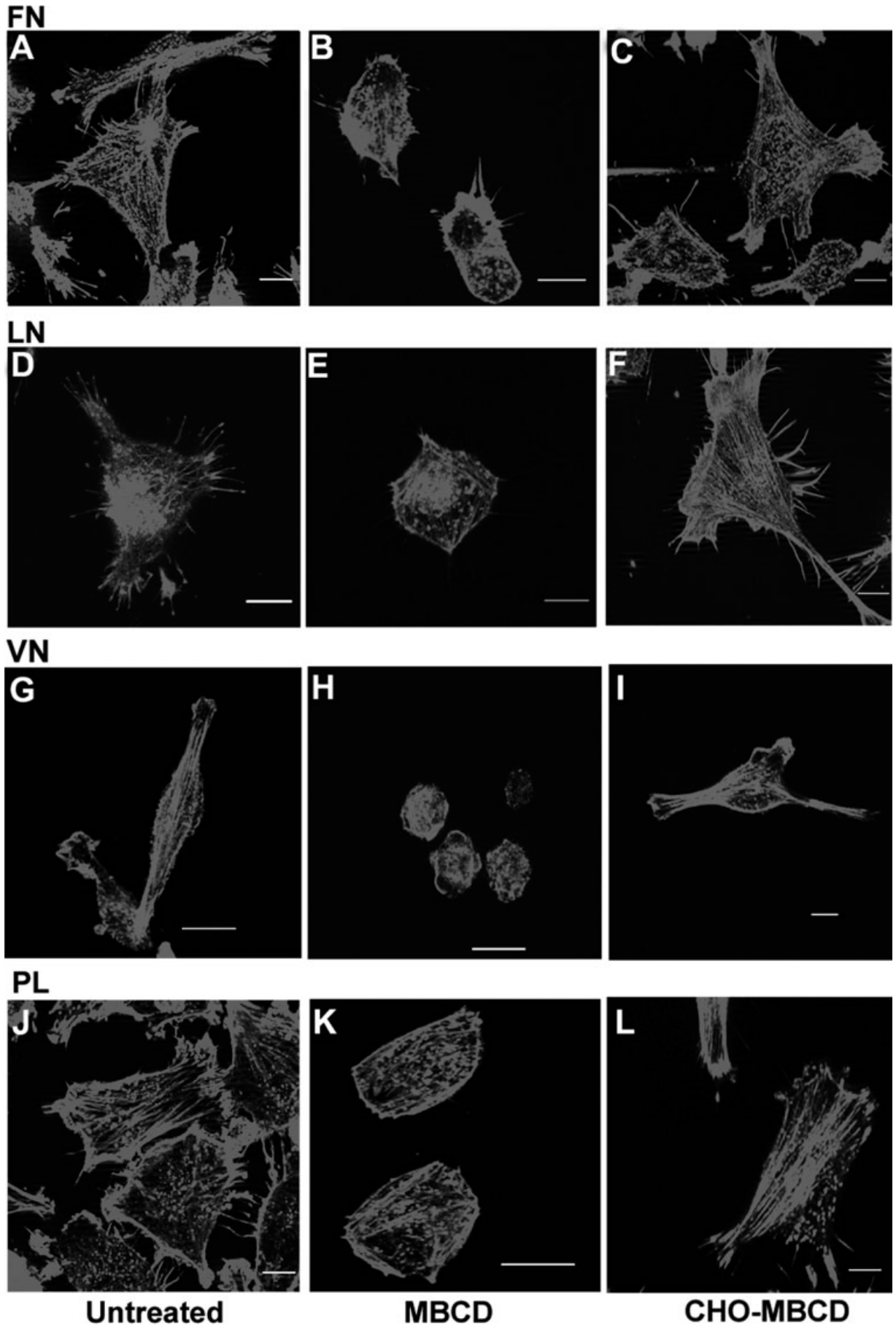

Figure 3.

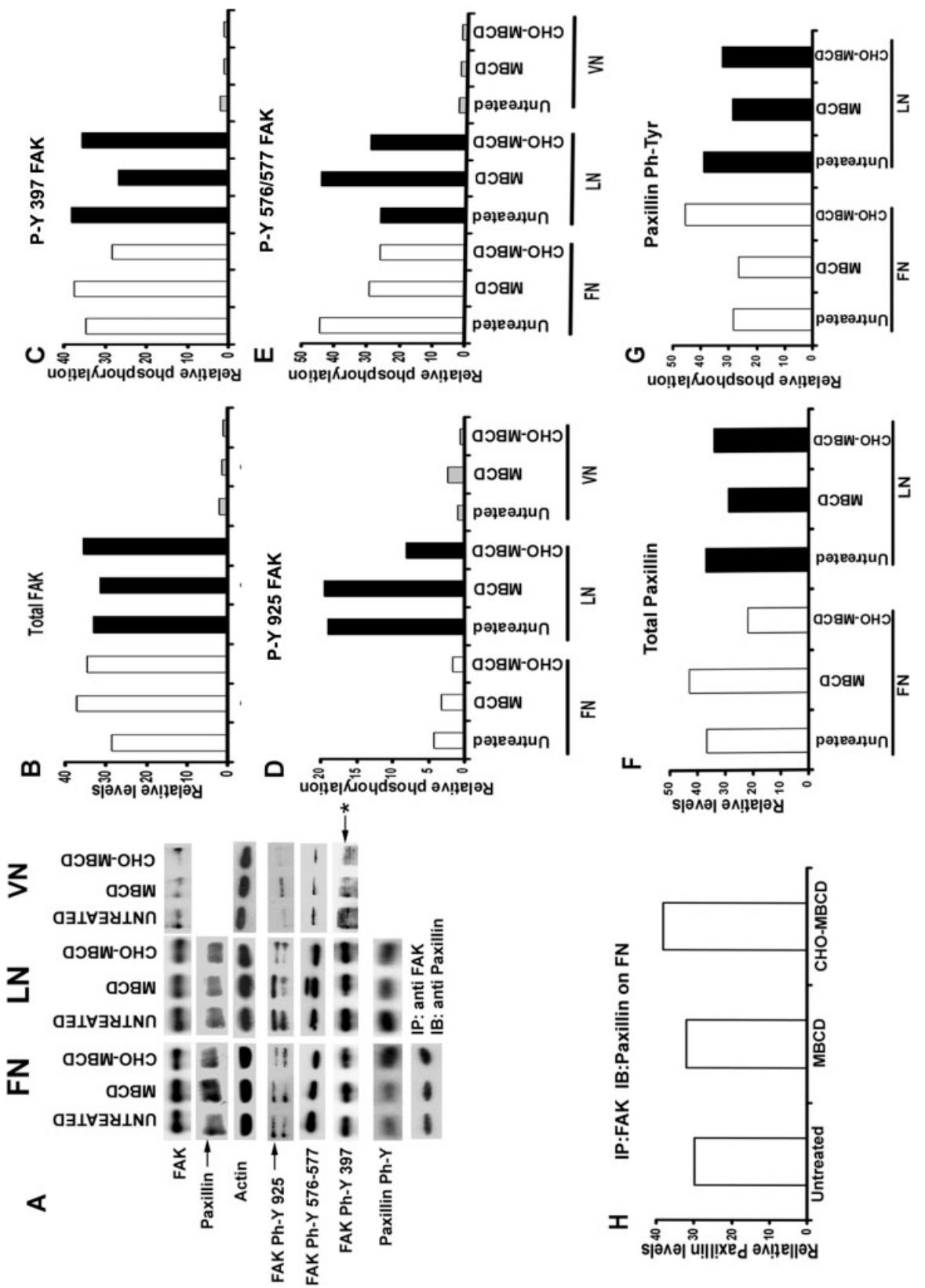
A
FN
LN
VN
UNTREATED
MBCD
CHO-MBCD
FAK
Paxillin
Actin
FAK Ph-Y 925
FAK Ph-Y 576-577
FAK Ph-Y 397
Paxillin Ph-Y
IP: anti FAK
IB: anti Paxillin
B
Total FAK
Relative levels
C
P-Y 397 FAK
Relative phosphorylation
D
P-Y 925 FAK
Relative phosphorylation
E
P-Y 576/577 FAK
Relative phosphorylation
F
Total Paxillin
Relative levels
G
Paxillin Ph-Tyr
Relative phosphorylation
Untreated
MBCD
CHO-MBCD
FN
LN
VN
H
IP:FAK IB:Paxillin on FN
Relative Paxillin levels
Untreated
MBCD
CHO-MBCD

Figure 4.

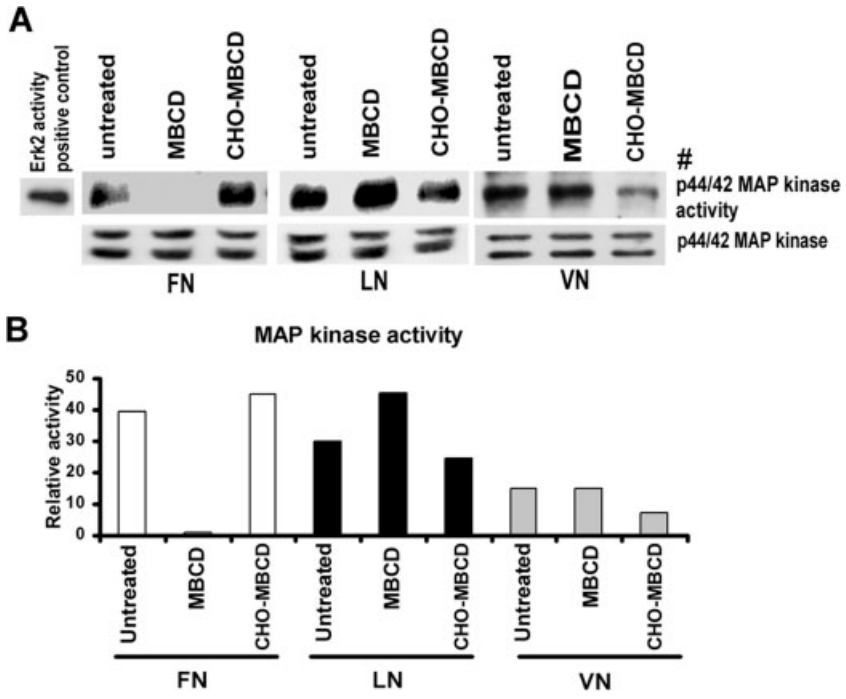

Fig. 5. Levels and activation of p44/42 MAP kinase in L27 cells on different substrata. The untreated cells were plated on various substrata for a period of 20–25 min. For chol depletion, the untreated cells plated on the substratum were treated with MBCD for 30 min. For cholesterol restoration, the MBCD-treated cells were treated with CHO-MBCD for 2 h. (**A**), Western blot analysis of the total (lower panels) and active (upper panels) p44/42 MAP kinase from lysates of L27 cells plated on FN, LN or VN and the corresponding densitometric scans, (**B**). # indicates the phosphorylation of p44 MAP kinase alone (this band was used for scanning) in cells plated on VN, as shown by the western blots of lysates with anti-phospho p44/42 monoclonal antibody.

slightly following chol restoration (Figs. 4A and 4C, white bars). In cells plated on LN, P-Y397 FAK levels decreased after MBCD treatment, but restored to untreated levels after restoration of chol (Figs. 4A and 4C, black bars). In cells plated on VN, P-Y397 FAK levels were similar in all conditions, but were lower, by a factor of more than 30, than those in cells plated on FN and LN (Figs. 4A and 4C, gray bars). However, P- Y925 FAK levels were significantly lower in cells plated on FN and VN than in cells plated on LN, in all conditions (Fig. 4D). We also did not find any changes with P-S910 FAK levels in cells plated on FN and LN (data not shown). We investigated the direct association of FAK with Pax in cells plated on FN, and found that the removal and restoration of cholesterol had no major effect on the FAK-Pax association (Figs. 4A and 4H).

MAP kinase (Erk1/2) levels in cells plated on FN, VN or LN were similar in all conditions (Fig. 5A, lower panels), but the phosphorylation of this protein was significantly reduced by chol depletion in cells plated on FN but slightly increased by chol depletion in cells palted on LN. Following the restoration of chol levels, Erk1/2 phosphorylation returned to basal levels on both surfaces. Interestingly, on VN-coated surfaces, only one of the two bands of the Erk1/2 complex (p44 MAPkinase) displayed phosphorylation, which was unaffected by MBCD treatment but decreased during chol restoration (Fig. 5A).

Thus, the changes in cell shape and motility described above may be due to changes in the activity of FAK and its effect on integrin-dependent downstream events involved in cytoskeletal organization.

Relocalization of α5β1 Integrin and Pax During Chol Modulation

We analyzed changes in the distribution of α5β1 integrin and Pax in L27 cells plated on FN. We examined the distribution and co-localization of α5β1 integrin and Pax by 2-color immunofluorescence confocal microscopy (Fig. 6). In untreated cells, α5 integrin (in green) was present in adhesion sites at the cell periphery and more centrally. At the periphery, some colocaliza-

Fig. 4. Expression levels and phosphorylation of FAK and Pax in L27 cells on different substrata. (**A**), Western blot analysis of cell lysates obtained from L27 cells plated on FN and LN, using anti-Pax antibodies, and for lysates obtained from cells plated on FN, LN or VN, using anti-FAK antibodies, under various chol conditions. Anti-actin blots were used as a loading control. The Pax antibody bound to two bands, the upper one of which (indicated by an arrow) corresponds to the intact Pax protein, which was used for densitometric scanning. Densitometric scans of the representative blots in this figure show relative amounts for total protein and the phosphorylation of FAK on specific tyrosine residues (**B** and **C–E**, respectively) and the whole Pax protein, (**F**) and tyrosine-phosphorylated Pax, (**G**). Direct association of FAK with Pax in cells plated on FN, as shown by immunoprecipitating the cell lysates with anti-FAK antibody, followed by western blotting with anti-Pax antibody (A, lower panel) and the corresponding densitometric scan, (**H**). * indicates the P-Y397 FAK band on VN, which was also used for densitometric scanning.

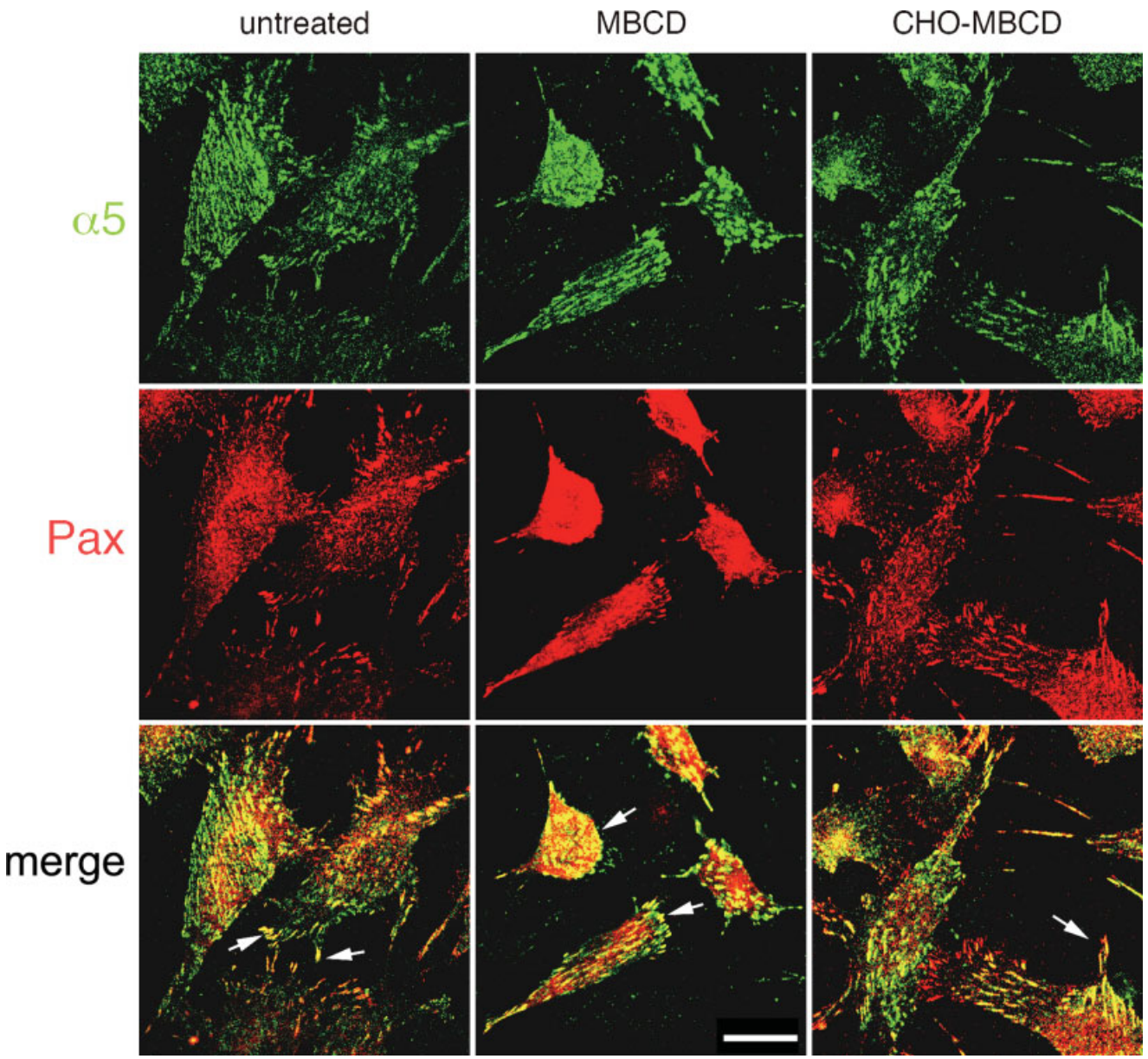

Fig. 6. Colocalization of α5 integrin and Pax in L27 cells. Localization of α5 integrin (upper panels) and Pax (middle panels) in L27 cells plated on FN, before (left row), after 1 h of MBCD treatment (middle row) and 2 h of CHO-MBCD treatment (right row). The arrows indicate the regions of colocalization on the merged images (lower panels). Bar, 10 μm.

Fig. 7. Dynamics of GFP-Paxillin and GFP-α5 integrin. (**A**), Individual frames of the time-lapse movie of L27 cells plated on FN transiently expressing GFP-Pax. The frames, taken at three-minute intervals, show the position of GFP-Pax in a representative untreated, MBCD-treated and CHO-MBCD-treated (for 30 min) cell. The arrows in (A) indicate dynamic Pax-rich adhesion sites (left panels), their coalescence into more centrally located sites under chol depletion (A, middle panels) and the reformation of the peripheral Pax-rich sites under chol restoration (right panels). Bar, 10 μm. (**B**), Individual frames from the time-lapse movie of a representative S180 cell plated on FN, transiently expressing α5-GFP integrin. The frames, taken at 5-min intervals for untreated and CHO-MBCD-treated (for 30 min) cells, and at 10-min intervals for MBCD-treated cells, show the position of the α5-GFP integrin. The arrows indicate the distribution of α5-GFP integrin in centrally (red arrows) or peripherally (white arrows) located sites or in vesicles (green arrows). For CHO-MBCD-treated cells, the arrows indicate the region of membrane ruffling and the absence of focal adhesion formation after 50 min of chol restoration. Bar, 10 mm.

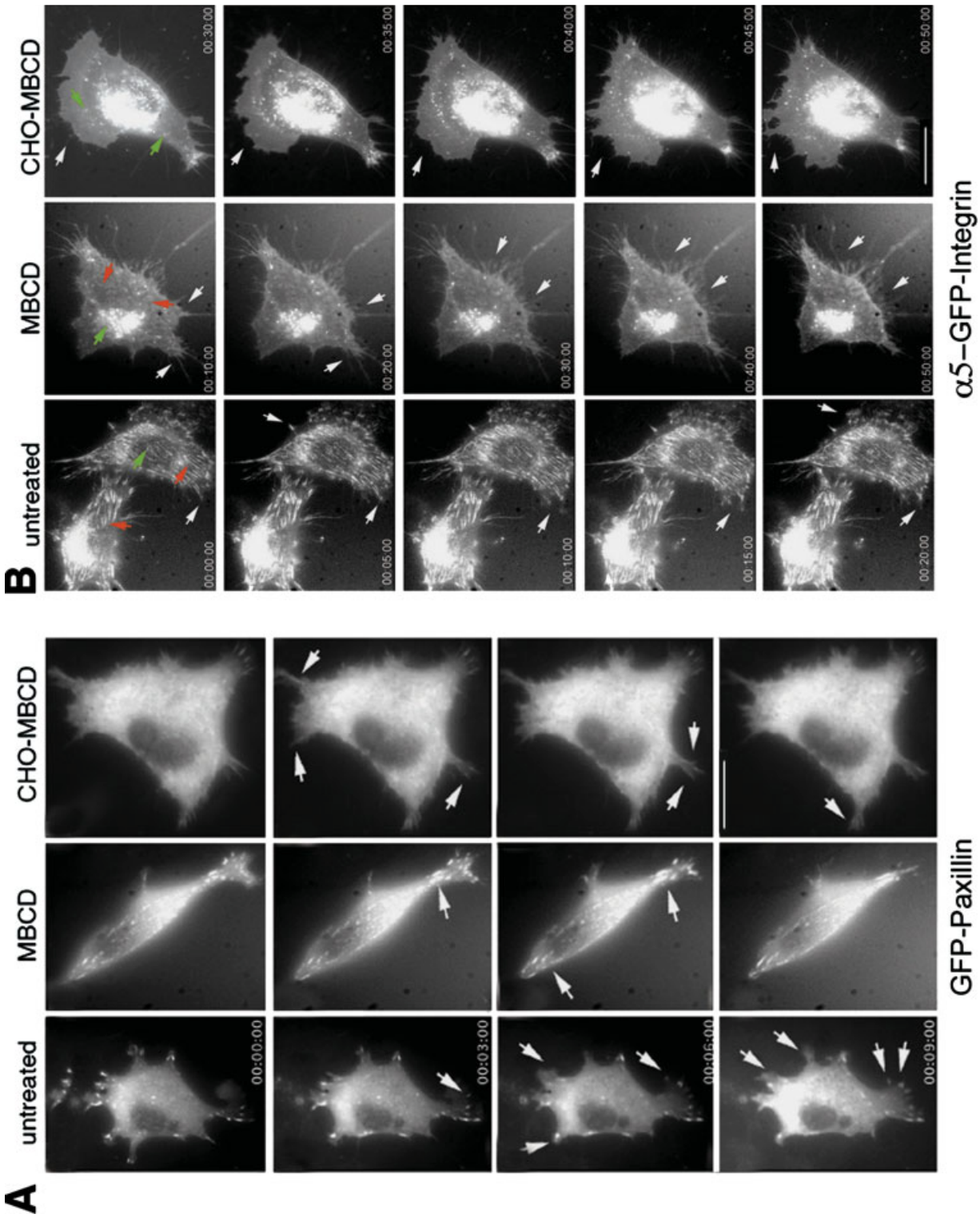
A
untreated
MBCD
CHO-MBCD
00:00:00
00:03:00
00:06:00
00:09:00
GFP-Paxillin
B
untreated
MBCD
CHO-MBCD
00:00:00
00:05:00
00:10:00
00:15:00
00:20:00
00:10:00
00:20:00
00:30:00
00:40:00
00:50:00
00:30:00
00:35:00
00:40:00
00:45:00
00:50:00
α5–GFP-Integrin

Figure 7.

tion of α5 integrin with Pax (in red) was observed in the lamellipodia, as shown by the yellow color in merged images. Some adhesion sites at the cell periphery displayed staining for Pax, but not α5 integrin, whereas central sites contained α5 integrin but not Pax. These observations were characteristic of focal contacts and fibrillar adhesions, respectively.

In cells plated on FN, the co-localization of Pax with α5 integrin increased significantly on MBCD treatment. In chol-restored cells, lower levels of α5 integrin and Pax colocalization were observed and the relocalization of molecules in the peripheral adhesions was observed. However, no lamellipodial colocalization of Pax and α5 integrin was seen in these cells.

An analysis of GFP-Pax localization in transiently transfected L27 cells plated on FN showed newly formed Pax-rich adhesion sites at the periphery of lamellipodia (Fig. 7A) to be dynamic in control conditions. By contrast, they progressively coalesced within more central sites during MBCD treatment and rounding up of cells. During chol restoration, new lamellipodia extended and GFP-Pax was relocated to the periphery, but the adhesion sites formed remained less dynamic than those in the control.

The dynamics and re-localization of α5 integrin were also studied by time-lapse videography of transiently transfected S180 parental cells with a construct encoding α5-GFP integrin, plated on FN-coated coverslips (Fig. 7B). In untreated cells, α5-GFP integrin was found in the cell membrane and was concentrated more at centrally located adhesion points, giving streaks. Some α5-GFP integrin was also seen in cytoplasmic vesicles or at peripheral adhesion sites, which were more dynamic than the central sites. During MBCD treatment, the membrane detached from the adhesion points, the cell became rounded and pieces of membrane containing α5-GFP integrin remained attached to the substratum along the path followed by the cell. The fluorescence of α5-GFP integrin decreased at the membranes, but some central α5-GFP integrin-positive sites were still observed. The overall level of α5 integrin at the cell surface decreased slightly during MBCD treatment, as shown by FACS analysis (Fig. 1B). The whole process of cell rounding took about 50 min. After MBCD treatment, the α5-GFP integrin-positive vesicles moved away from the membrane, toward the Golgi network. The cells spread out again on chol restoration, but α5-GFP integrin relocalized less strongly at adhesion sites, giving a pattern different from that observed in untreated cells. The cells began to spread out again after 30 min of CHO-MBCD treatment and this spreading became more pronounced after 2 h (not shown). During the course of membrane chol restoration, the α5-GFP integrin vesicles moved toward the membrane.

We analyzed the distribution of α5β1 integrin and Pax in sucrose density gradients. In untreated L27 cells plated on FN, (supplementary data S9A) integrin molecules were detected in all the fractions, whereas Pax was restricted to the high density (45% sucrose) fractions (fractions 6–10). The same pattern was observed for MBCD-treated L27 cells plated on FN (supplementary data S9B). With chol restoration (supplementary data S9C), the distribution of integrin remained similar to that in MBCD-treated cells, whereas Pax crossed the 45% sucrose barrier into the 6th fraction, corresponding to 35% sucrose.

DISCUSSION

Integrins and ECM proteins play an important role in regulating the shape and motility of mammalian cells [Hynes, 2002]. Specific interactions between integrins and their ligands elicit a large number of signaling responses, affecting many cell properties, such as shape, locomotion, survival and division [Miranti and Brugge, 2002; Stupack and Cheresh, 2002]. Chol modulates integrin functions [Gopalakrishna et al., 2000], and regulates the thickness and the curvature of model membranes [Rukmini et al., 2001; Gallova et al., 2004], indicating a more general role in the transmission of signaling responses through adhesion receptors. Our results indicate that membrane chol can modify the α5β1 integrin- and FN-mediated signaling pathways that are known to regulate cell shape, adhesion and motility. The following points highlight the significance of our observations.

Role of Plasma Membrane Cholesterol in Controlling Cell Shape and Motility

The presence of chol in the plasma membrane is important for membrane rigidity/fluidity, the organization of specific domains and the regulation of signaling responses [Simons and Toomre, 2000]. Chol has been reported to be involved in the redistribution of raft domains during signaling in chemotactic cells [Gomez-Mouton et al., 2004] and in the regulation of nerve growth cone guidance [Guirland et al., 2004]. Chol has also been shown to modify the adhesion and growth of cells [Kaur et al., 2004]. A few reports have indicated a possible role for chol in regulating cell motility [Ghosh et al., 2002; Pierini et al., 2003], but its role in controlling cell shape and adhesion remains unclear.

We show here that the acute depletion and restoration of chol levels in cells (Fig. 1A) containing significant amounts of α5β1 integrin (S2 B) cause fully reversible changes in cell adhesion to FN (Figs. 1D–1F), and far less reversible changes in cell motility (Fig. 2A). The changes in both these properties of the cell occur in the absence of a significant change in either the level or the

state of activation of the integrin (Figs. 1B and 1C). Comparison of these data with the behavior of L27 cells on LN, VN and uncoated PL surfaces showed that the modification of chol levels in the membrane regulated cell adhesion to all surfaces, except VN (Figs. 1D–1L). However, the single largest change in cell motility was recorded for cells plated on FN, with a 65% decrease in motility recorded for cells depleted of chol and a partial recovery upon chol restoration, to levels 50% those in untreated cells (Fig. 2A). These changes may reflect the nature of the integrins and signaling mechanisms involved and their sensitivity to chol in the regulation cell motility on FN, LN and VN.

We also observed substrate-specific differences in the effects of chol removal on cell shape (compare the panels in Fig. 2B and Supplementary Data S4-S7). L27 cells plated on FN tended to spread horizontally. They became more rounded after the removal of chol and then spread out again when chol levels were restored. However, the cells did not spread out much on LN from the outset and, on this surface, they rapidly became rounded when chol was removed and did not spread out again, even after 3 h of chol restoration (Movie S5). On VN, the cells spread out, but less extensively than on FN, with more membrane ruffling observed in the smaller lamellipodia in untreated cells (Movie S6). Further analysis indicated that these differences in cell shape and motility were due to the differences in the distribution of F-actin in these cells under different membrane chol conditions. Only a few studies have focused on the substrate-specific changes in cell shape induced by chol. Kwik et al. [2003] reported no significant changes in cell shape after chol removal in human skin fibroblasts plated on PL. We also observed little change in the shape of L27 cells plated on PL (Figs. 2E and 3), whereas robust changes were observed in cells plated on FN, indicating that chol removal affects cell shape in a substrate-specific manner.

D711 cells (overexpressing $\alpha 4\beta 1$ integrin, another FN-specific integrin) displayed no significant change in cell motility on FN, LN and PL when cholesterol was removed and restored (Supplementary data S8A). They displayed a clear shape change in response to cholesterol removal or restoration only when plated on FN (Supplementary data S8B). This highlights the fact that cholesterol mediated changes in cell motility and shape are prominent only for cells overexpressing $\alpha 5$ integrin and plated on FN.

Cytoskeletal F-Actin and the Influence of Membrane Chol

The actin-based cytoskeleton and its various organizations—focal adhesion-attached stress fibers, cortical actin, growing and retracting actin filaments (F-actin), unpolymerized globular actin (G-actin) etc.—play an important role in determining the shape and motility of cells [Small et al., 2002; Suetsugu and Takenawa, 2003]. F-actin also regulates the formation of lamellipodial and filopodial extensions of the cell membrane [Raftopoulou and Hall, 2004; Vallotton et al., 2004] and can remodel membrane microdomains [Burgstaller and Gimona, 2003]. Chol-determined plasma membrane microviscosity (PMM) and the modulation of PMM have been shown to favor lamellipodial extension in migrating endothelial cells [Vasanji et al., 2004]. The role of chol in all these processes has been reviewed elsewhere [Manes and Martinez, 2004]. Chol is not thought to affect the actin polymerization machinery directly. Instead, it stabilizes the F-actin meshwork and membrane stiffness at the leading edge of lamellipodia.

Our results concerning the organization and distribution of F-actin in cells during chol depletion and restoration are consistent with these observations. However, we observed different distributions of F-actin in cells plated on different substrata (Fig. 3). Cells plated on FN and PL displayed robust stress fiber formation. Following chol removal, the stress fibers totally disappeared and actin adopted a cortical distribution in cells plated on FN, whereas residual stress fibers were observed in cells plated on PL. L27 cells plated on LN and VN displayed no stress fiber formation, and even the cortical redistribution of actin was less marked in MBCD-treated cells. However, robust stress fibers did form during chol restoration. We also observed differences between cells plated on FN, LN and VN in terms of the distribution of actin in lamellipodia and filopodia, with filopodia more common in cells plated on LN and lamellipodium formation more common in cells plated on FN and uncoated PL. This difference correlates well with the migratory properties of cells on FN, VN and LN — cells move faster on FN than on LN or VN. The actin cytoskeleton has been shown to regulate cell motility by continuous polymerization and branching at the leading edge of the F-actin meshwork in a growing lamellipodium, accompanied by the depolymerization of actin at the trailing end of the same meshwork [Giannone et al., 2004]. In our cells, these areas were free of stress fibers, but Pax-rich focal adhesions were observed (Figs. 6 and 7A). Actin fibers are arranged in parallel in filopodia, which do not contain focal adhesions. Thus, lamellipodia facilitate cell motility on FN, but not on LN or VN, due to their smaller size and number. In MBCD-treated cells on FN, the lamellipodia disappear and actin adopts a cortical distribution, becoming more closely apposed to the plasma membrane, possibly leading to higher cortical tension in the membrane and decreasing cell motility. Chol restoration leads to the reappearance of actin stress fibers, but few lamellipodia are observed, resulting in

restoration of the initial well spread morphology of cells. However, the cells are less motile than they were originally. We looked at the levels of rhoA protein and its GTP binding activity, but no differences were observed between the three sets of conditions (data not shown).

Regulation of MAP Kinase Erk1/2, FAK and Pax by Chol

Our results clearly show that Erk1/2 MAP kinase activity is decreased by the depletion of chol from L27 cells plated on FN (Fig. 5A). By contrast, Erk1/2 increased slightly after chol depletion in cells plated on LN. Erk1/2 kinase activity regulates FAK phosphorylation at serine 910 [Hunger-Glaser et al., 2003; Schlaepfer and Mitra, 2004], reducing the binding of Pax to FAK and affecting cell motility. However, we observed no change in the association between FAK and Pax (Figs. 4A and 4H), implying that FAK phosphorylation at serine 910 was not affected by chol removal and restoration. The significance of Erk1/2 dephosphorylation upon chol removal may concern another property of FAK or another molecule involved in the pathway regulating motility.

Several reviews [Schlaepfer and Mitra, 2004; Mitra et al., 2005] have evaluated the effects of phosphorylation of different tyrosine and serine residues in FAK on the signaling pathway controlling cell spreading, adhesion and motility. The phosphorylation of P-Y397 FAK, situated in the N-terminal domain of the molecule, is a critical modification of FAK, resulting in the localization of FAK to focal adhesions [Ruest et al., 2000]. We observed no change in the phosphorylation of Y397 (Figs. 4A and 4C), indicating that this modification is not involved in chol-regulated changes in cell shape and motility. These data on Y397 FAK phosphorylation are consistent with our confocal microscopy observations, in which no changes in FAK localization in focal adhesions were observed (not shown). Phosphorylation of the Y576/577 residues of FAK is also important for the hyperphosphorylation of FAK and maintenance of the optimal phosphorylation status of this protein [Leu and Maa, 2002]. As tyrosine residues 576 and 577 are located within the catalytic domain of the FAK molecule, changes in the phosphorylation status of these residues also affect the adhesion-induced signaling of the downstream targets of FAK [Parsons, 2003]. In our experiments, chol elimination decreased Y576/577 phosphorylation on FN (Figs. 4A and 4E, white bars). This finding is consistent with the lower motility of cells on FN after chol removal (Fig. 2A), indicating a positive correlation between FAK Y576/577 phosphorylation and higher cell motility, consistent with the findings of other studies [Nakamura et al., 2001]. FAK phosphorylation at Y925 regulates the binding of FAK to Pax and the dissociation of FAK from focal adhesions [Liu et al., 2002; Katz et al., 2003]. Levels of FAK Y925 phosphorylation were very low in cells plated on FN, and remained so in all chol conditions (Figs. 4A and 4D, white bars). The association of FAK with Pax was also unaffected, indicating that Pax can bind FAK even if its level of phosphorylation is very low. Thus, we observed substrate-specific changes in the phosphorylation of specific tyrosine residues of FAK upon chol modulation. However, it is unclear which change in the activity of FAK is responsible for the lower adhesion and motility of L27 cells on FN and the little change on LN. Nonetheless, FAK emerges as the major target of the chol-regulated signaling controlling cell adhesion, shape and locomotion. Further studies are required to determine the role of FAK more precisely in this process.

It should also be borne in mind that, in our experiments on Pax phosphorylation, we observed no significant change in overall or phosphorylated Pax levels when chol was removed (Figs. 4A, 4F and 4G). However, time lapse analyses of the distribution of Pax (Fig. 7A) showed that Pax was relocated to adhesion sites at the center of the cell after chol removal, returning to the periphery after chol restoration. In all membrane chol conditions, some Pax molecules were colocalized with $\alpha5\beta1$ integrin, but the extent of this colocalization depended on the level of chol in the membrane (Fig. 6). This observation may be important, given the differences previously observed in the association of Pax with focal adhesions in motile and non-motile cells [Zamir et al., 2000; Nakamura et al., 2001]. The movement of integrin and Pax molecules away from the peripheral focal adhesions after chol depletion may also be facilitated by the depolymerization of actin stress fibers, as shown in a different context [Laukaitis et al., 2001].

Effects of Chol on the Distribution of Integrin and Pax

Chol is known to play an important role in the formation of membrane domains (rafts) that may harbor specific lipid and protein molecules, including molecules involved in cell signaling in general [Brown and London, 2000; Simons and Toomre, 2000], and integrins in particular [Guan, 2004]. The domain/raft-specific behavior of $\alpha3\beta1$ and its protein partners and of $\alpha6\beta4$ integrins has been described [Hemler, 2003; Gagnoux-Palacios et al., 2003].

We have investigated the distribution of $\alpha5\beta1$ integrin and Pax in the plasma membrane of L27 cells plated on FN under different chol conditions. We found no difference in the distribution of $\alpha5\beta1$ integrin in detergent-resistant fractions of the plasma membrane, and this integrin was found to be uniformly distributed among all fractions (Supplementary data S9). This pattern of $\alpha5\beta1$-integrin distribution was not affected by the elimination of chol from the membrane, or its reintroduction. Pax was restricted to heavier fractions—

those least resistant to detergents—and even this pattern was not affected by treatment with MBCD and CHO-MBCD (S9). Under the same conditions, the distribution of caveolin-1, a raft-specific marker, was also unaffected (data not shown). Since the protein distributions were not altered, we believe that the changes in adhesion and motility are not related to the composition of membrane rafts. These results are also consistent with the persistent colocalization of the two molecules in different chol conditions. The movement of Pax and α5β1 integrin in time-lapse analyses (Figs. 7A and 7B) suggests that the integrin and Pax molecules that move to the center of the cell are those from the heavier fractions of the gradient, whereas integrin molecules shed from the membrane or internalized are not associated with Pax.

In summary, we have shown that chol plays a significant role in regulating the cell shape, adhesion and migration of cells plated on FN and that its effects are mediated by changes in the organization of the actin cytoskeleton. Chol-mediated signaling involving FAK and Erk1/2 MAP kinases plays a key role in this process, but a more specific mechanism involving these two intricately linked adhesion and motility regulators remains to be established.

ACKNOWLEDGMENTS

We thank J.-B. Sibarita, V. Fraisier, D. Meur and D. Morineau for assistance with imaging and computerized video microscopy. We thank M. Hemler, K. M. Yamada and C. Stipp for their suggestions at various stages of this study. PJ and KSR held IFCPAR postdoctoral fellowships. OGR held a predoctoral fellowship from the University Grants Commission, India.

REFERENCES

Akiyama SK, Yamada SS, Chen WT, Yamada KM. 1989. Analysis of fibronectin receptor function with monoclonal antibodies: Roles in cell adhesion, migration, matrix assembly, and cytoskeletal organization. J Cell Biol 109:863–875.

Beauvais A, Erickson CA, Goins T, Craig SE, Humphries MJ, Thiery JP, Dufour S. 1995. Changes in the fibronectin-specific integrin expression pattern modify the migratory behaviour of sarcoma S180 Cells *in vitro* and in the embryonic environment. J Cell Biol 128:699–713.

Blystone SD. 2004. Integrating an integrin: A direct route to actin. Biochim Biophys Acta 1692:47–54.

Bokoch GM. 2003. Biology of the p21-activated kinases. Annu Rev Biochem 15:1904–1917.

Brown DA, London E. 2000. Structure and function of sphingolipid and cholesterol-rich membrane rafts. J Biol Chem 275:17221–17224.

Brown MC, Turner CE. 2004. Paxillin: Adapting to change. Physiol Rev 84:1315–1339.

Burgstaller G, Gimona M. 2003. Actin cytoskeleton remodelling via local inhibition of contractility at discrete microdomains. J Cell Sci 117:223–231.

Claas C, Stipp CS, Hemler ME. 2001. Evaluation of prototype transmembrane 4 superfamily protein complexes and their relation to lipid rafts. J Biol Chem 276:7974–7984.

Chen Z, Rand RP. 1997. The influence of cholesterol on phospholipid membrane curvature and bending elasticity. Biophys J 73:267–276.

Chu YS, Thomas WA, Eder O, Pincet F, Perez E, Thiery JP, Dufour S. 2004. Force measurements in E-cadherin-mediated cell doublets reveal rapid adhesion strengthened by actin cytoskeleton remodeling through Rac and Cdc42. J Cell Biol 167:1183–1194.

Defilippi P, van Hinsbergh V, Bertolotto A, Rossino P, Silengo L, Tarone G. 1991. Differential distribution and modulation expression of α1/β1 integrin on human endothelial cells. J Cell Biol 114:855–863.

Dufour S, Beauvais-Jouneau A, Delouvee A, Thiery JP. 1999. Differential function of *N*-cadherin and cadherin-7 in the control of embryonic cell motility. J Cell Biol 146:501–516.

Erickson CA, Tosney KW, Weston JA. 1980. Analysis of migratory behavior of neural crest and fibroblastic cells in embryonic tissues. Dev Biol 77:142–156.

Gagnoux-Palacios L, Dans M, van't Hof W, Mariotti A, Pepe A, Meneguzzi G, Resh MD, Giancotti FG. 2003. Compartmentalization of integrin α6β4 signalling in lipid rafts. J Cell Biol 162:1189–1196.

Gallova J, Uhrikova D, Islamov A, Kuklin A, Balgavy P. 2004. Effect of cholesterol on the bilayer thickness in unilamellar extruded DLPC and DOPC liposomes: SANS contrast variation study. Gen Physiol Biophys 23:113–128.

Geiger B, Bershadsky A, Pankov R, Yamada KM. 2001. Transmembrane extracellular matrix-cytoskeleton crosstalk. Nat Rev Mol Cell Biol 2:793–805.

Ghosh PK, Vasanji A, Murugesan G, Eppell SJ, Graham LM, Fox PL. 2002. Membrane microviscosity regulates endothelial cell motility. Nat Cell Biol 4:894–900.

Giancotti FG, Ruoslahti E. 1999. Integrin signalling. Science 285: 1028–1032.

Giannone G, Dubin-Thaler BJ, Dobereiner BJ, Kieffer N, Bresnick AR, Sheetz MP. 2004. Periodic lamellipodial contractions correlate with rearward actin waves. Cell 116:431–443.

Gomez-Mouton C, Lacalle RA, Mira E, Jimenez-Baranda S, Barber DF, Carrera AC, Martinez-A C, Manes S. 2004. Dynamic redistribution of raft domains as an organizing platform for signaling during chemotaxis. J Cell Biol 164:759–768.

Gopalakrishna P, Chaubey SK, Manogaran PS, Pande G. 2000. Modulation of α5β1 integrin functions by the phospholipid and cholesterol contents of cell membranes. J Cell Biochem 77:517–528.

Gopalakrishna P, Rangaraj N, Pande G. 2004. Cholesterol alters the interaction of glycosphingolipid GM3 with α5β1 integrin and increases integrin-mediated cell adhesion to fibronectin. Exp Cell Res 300:43–53.

Guan J. 2004. Integrins, rafts, rac, and rho. Science 303:773–774.

Guirland C, Suzuki S, Kojima M, Lu B, Zheng JQ. 2004. Lipid rafts mediate chemotropic guidance of nerve growth cones. Neuron 42:51–62.

Hemler ME. 2003. Tetraspanin proteins mediate cellular penetration, invasion, and fusion events and define a novel type of membrane microdomain. Annu Rev Cell Dev Biol 19:397–422.

Hunger-Glaser I, Salazar EP, Sinnett-Smith J, Rozengurt E. 2003. Bombesin, lysophosphatidic acid, and epidermal growth factor rapidly stimulate focal adhesion kinase phosphorylation at Ser-910: Requirement for ERK activation. J Biol Chem 278: 22631–22643.

Hynes RO. 2002. Integrins: Bidirectional, allosteric signalling machines. Cell 110:673–687.

Hynes RO, Marcantonio EE, Stepp MA, Urry LA, Yee GH. 1989. lntegrin heterodimer and receptor complexity in avian and mammalian cells. J Cell Biol 109:409–420.

Ingber DE. 2003a. Tensegrity. I. Cell structure and hierarchial systems biology. J Cell Sci 116:1157–1173.

Ingber DE. 2003b. Tensegrity. II. How structural networks influence cellular information processing networks. J Cell Sci 116:1397–1408.

Katz B, Romer L, Miyamoto S, Volberg T, Matsumoto K, Cukierman E, Geiger B, Yamada KM. 2003. Targeting membrane localized focal adhesion kinase to focal adhesions: Roles of tyrosine phosphorylation and SRC family kinases. J Biol Chem 278: 29115–29120.

Kaur T, Gopalakrishna P, Manogaran PS, Pande G. 2004. A correlation between membrane cholesterol level, cell adhesion and tumorigenecity of polyoma virus transformed cells. Mol Cell Biochem 265:83–95.

Kwik J, Boyle S, Fooksman D, Margolis L, Sheetz MP, Edidin M. 2003. Membrane cholesterol, lateral mobility, and the phosphatidylinositol 4,5-bisphosphate-dependent organization of cell actin. Proc Natl Acad Sci USA 100:13964–13969.

Laukaitis CM, Webb DJ, Donais K, Horwitz AF. 2001. Differential dynamics of α5 integrin, paxillin, and α-actinin during formation and disassembly of adhesions in migrating cells. J Cell Biol 153:1427–1440.

Leu TH, Maa MC. 2002. Tyr-863 phosphorylation enhances focal adhesion kinase autophosphorylation at Tyr-397. Oncogene 21: 6992–7000.

Ling K, Doughman RL, Firestone AJ, Bunce MW, Anderson RA. 2002. Type I gamma phosphatidylinositol phosphate kinase targets and regulates focal adhesions. Nature 420:89–93.

Liu G, Guibao CD, Zheng J. 2002. Structural insight into the mechanisms of targeting and signalling of focal adhesion kinase. Mol Cell Biol 22:2751–2760.

Manneville SE, Hall A. 2002. Rho GTPases in cell biology. Nature 420:629–635.

Manes S, Martínez AC. 2004. Cholesterol domains regulate the actin cytoskeleton at the leading edge of moving cells. Trends Cell Biol 14:275–278.

Miranti CK, Brugge JS. 2002. Sensing the environment: A historical perspective on integrin signal transduction. Nat Cell Biol 4:83–90.

Mitra SK, Hanson DA, Schlaepfer DD. 2005. Focal adhesion kinase: In command and control of cell motility. Nat Rev Mol Cell Biol 6:56–68.

Nakamura K, Yano H, Schaefer E, Sabe H. 2001. Different modes and qualities of tyrosine phosphorylation of FAK and Pyk2 during epithelial-mesenchymal transdifferentiation and cell migration: Analysis of specific phosphorylation events using site-directed antibodies. Oncogene 20:2626–2635.

Pande G. 2000. The role of membrane lipids in regulation of integrin functions. Curr Opin Cell Biol 12:569–574.

Parsons JT. 2003. Focal adhesion kinase: The first ten years. J Cell Sci 116:1409–1416.

Pierini LM, Eddy RJ, Fuortes M, Seveau S, Casulo C, Maxfield FR. 2003. Membrane lipid organization is critical for human neutrophil polarization. J Biol Chem 278:10831–10841.

Rafelski SM, Theriot JA. 2004. Crawling toward a unified model of cell motility: Spatial and temporal regulation of actin dynamics. Annu Rev Biochem 73:209–239.

Raftopoulou M, Hall A. 2004. Cell migration: Rho GTPases lead the way. Dev Biol 265:23–32.

Ridley AJ, Schwartz MA, Burridge K, Firtel RA, Ginsberg MH, Borisy G, Parsons JT, Horwitz AR. 2003. Cell migration: Integrating signals from front to back. Science 302:1704–1709.

Rossino P, Gavazzi I, Timpl R, Aumailley M, Abbadini M, Giancotti F, Silengo L, Marchisio PC, Tarone G. 1990. Nerve growth factor induces increased expression of a laminin-binding integrin in rat pheochromocytoma PC12 cells. Exp Cell Res 189:100–108.

Ruest PJ, Roy S, Shi E, Mernaugh RI, Hanks SK. 2000. Phosphospecific antibodies reveal focal adhesion kinase activation loop phosphorylation in nascent and mature focal adhesions and requirement for the autophosphorylation site. Cell Growth Differ 11:41–48.

Rukmini R, Rawat SS, Biswas SC, Chattopadhyay A. 2001. Cholesterol organization in membranes at low concentrations: Effects of curvature stress and membrane thickness. Biophys J 81: 2122–2134.

Schaller MD. 2004. FAK and paxillin: Regulators of *N*-cadherin adhesion and inhibitors of cell migration? J Cell Biol 166:157–159.

Schlaepfer DD, Mitra SK. 2004. Multiple connections link FAK to cell motility and invasion. Curr Opin Gen Dev 14:92–101.

Simons K, Toomre D. 2000. Lipid rafts and signal transduction. Nat Rev Mol Cell Biol 1:31–39.

Small JV, Stradal T, Vignal E, Rottner K. 2002. The lamellipodium: Where motility begins. Trends Cell Biol 12:112–120.

Stupack DG, Cheresh DA. 2002. Get a ligand, get a life: Integrins, signalling and cell survival. J Cell Sci 115:3729–3738.

Suetsugu S, Takenawa T. 2003. Regulation of cortical actin networks in cell migration. Int Rev Cytol 229:245–286.

Vallotton P, Gupton SL, Waterman-Storer CM, Danuser G. 2004. Simultaneous mapping of filamentous actin flow and turnover in migrating cells by quantitative fluorescent speckle microscopy. Proc Natl Acad Sci USA 101:9660–9665.

Vasanji A, Ghosh PK, Graham LM, Eppell SJ, Fox PL. 2004. Polarization of plasma membrane microviscosity during endothelial cell migration. Dev Cell 6:29–41.

Yang X, Kovalenko OV, Tang W, Claas C, Stipp CS, Hemler ME. 2004. Palmitoylation supports assembly and function of integrin-tetraspanin complexes. J Cell Biol 167:1231–1240.

Zamir E, Geiger B. 2001. Molecular complexity and dynamics of cell-matrix adhesions. J Cell Sci 114:3583–3590.

Zamir E, Katz M, Posen Y, Erez N, Yamada KM, Katz BZ, Lin S, Lin DC, Bershadsky A, Kam Z, Geiger B. 2000. Dynamics and segregation of cell-matrix adhesions in cultured fibroblasts. Nat Cell Biol 2:191–197.